

# X-ray microdiffraction and conventional diffraction from frozen-hydrated biological specimens

Hiroyuki Iwamoto,<sup>a\*</sup> Katsuaki Inoue,<sup>a</sup> Tetsuro Fujisawa<sup>b</sup> and Naoto Yagi<sup>a</sup><sup>a</sup>Research and Utilization Division, SPring-8, Japan Synchrotron Radiation Research Institute, Hyogo 679-5198, Japan, and <sup>b</sup>Structural Biochemistry Laboratory, RIKEN Harima Institute, SPring-8, Hyogo 679-5148, Japan. E-mail: iwamoto@spring8.or.jp

Received 7 March 2005

Accepted 28 April 2005

A system for recording microdiffraction patterns from micrometer-sized quick-frozen hydrated biological specimens at the high-flux beamline BL40XU of SPring-8 is described. The optics consists of a pair of pinholes drilled into tantalum substratum, with a defining aperture of diameter 2  $\mu\text{m}$ . The frozen specimens are placed in an in-vacuum cryochamber mounted on a three-axis goniometer, where the specimens are stably held at a liquid-nitrogen temperature ( $\sim 74$  K). A beam size of 1.5  $\mu\text{m}$  (full width at half-maximum) is attained at the sample position. By using this system, diffraction patterns have been recorded from an isolated single myofibril (diameter  $\sim 3$   $\mu\text{m}$ ) of an insect flight muscle in an area equivalent to a single sarcomere (length  $\sim 3$   $\mu\text{m}$ ). The technique is potentially applicable to other micrometer-sized hydrated biological specimens, which are more susceptible to radiation damage than dry synthetic polymers or biopolymers. The quick-freezing of biological specimens has also been proven useful in reducing the specimen volume in the beam in conventional diffraction recordings.

© 2005 International Union of Crystallography  
Printed in Great Britain – all rights reserved**Keywords:** microbeam; single myofibril; single sarcomere; liquid-nitrogen temperature.

## 1. Introduction

Since the advent of the third-generation synchrotron radiation sources, diffraction recordings using micrometer-sized X-ray beams (X-ray microbeams) have proven useful in a wide range of applications for materials and biological sciences. A variety of biological specimens (*e.g.* collagen, human hair, bird feather, silks spun by various arthropod animals, lipid multilayers; Busson *et al.*, 1999; Kreplak *et al.*, 2002; Lichtenegger *et al.*, 1999; Riekel *et al.*, 2000; Rossle *et al.*, 2004) have been subjected to microbeam diffraction analysis, again by using a variety of microbeam optics (pinhole arrays, tapered capillaries, waveguides, Fresnel zone plates *etc.*). [An excellent review has been presented by Ice (1997). See also Tamura *et al.* (2003).] Living or membrane-permeabilized cells or organelles isolated from them are also expected to be potential materials for microdiffraction analysis, but they are more difficult to handle because of their fragility, greater susceptibility to radiation damage and weaker diffraction intensities.

The earliest example of microbeam recording from such (unfrozen) hydrated biological specimens is diffraction recording from single myofibrils of insect flight muscle using 2  $\mu\text{m}$  pinholes (Iwamoto, Nishikawa *et al.*, 2002). Clearly defined reflection spots were recorded, and they were indexable to the hexagonal array of myofilaments. However, the specimens were unstable, and not many diffraction patterns

were recorded until the enzyme substrate (ATP) was consumed and the specimens finally started to dehydrate.

It is expected that the stability of such hydrated biological specimens will be greatly improved if they are frozen and kept at low temperature throughout the recording. The specimen must be quick-frozen to prevent the formation of ice crystals that would destroy the fine structures to be studied. Here we describe the method to prepare quick-frozen biological specimens suitable for microdiffraction, and the optical set-up for diffraction recordings from the specimen kept at the liquid-nitrogen temperature. The specimen volume in the original work (Iwamoto, Nishikawa *et al.*, 2002) was  $\sim 2$   $\mu\text{m}$  diameter  $\times$   $\sim 3$  mm length ( $\sim 10000$   $\mu\text{m}^3$  or  $\sim 1000$  sarcomeres in series). By quick-freezing the specimen, the volume has been reduced to  $\sim 2$   $\mu\text{m}$  diameter  $\times$   $\sim 3$   $\mu\text{m}$  length ( $\sim 10$   $\mu\text{m}^3$  or equivalent to a single sarcomere), representing a 1000-fold gain. An example of the application of this quick-freezing and recording-while-frozen technique to conventionally sized specimen (single muscle fibers) is also described.

## 2. Methods

### 2.1. X-ray optics and sample stage

For microdiffraction, quasi-monochromatic X-ray beams were used at the high-flux beamline BL40XU of SPring-8

(Inoue *et al.*, 2001). The energy of the beam was 12.4 keV and its resolution was  $\sim 2\%$ . The beams were attenuated to 1/100 by using a fast-rotating tantalum disc with slit openings before they were led to the pinhole optics. The pinhole optics and the sample stage were built into a single unit (Fig. 1). The pinhole optics similar to that described by Iwamoto, Nishikawa *et al.* (2002) consisted of two pinholes drilled into 50  $\mu\text{m}$ -thick tantalum substratum (custom-made by Lenox Laser, Glen Arm, USA). The upstream defining pinhole had an aperture of diameter 2  $\mu\text{m}$ , while that of the downstream guard pinhole was 10  $\mu\text{m}$  in diameter. Immediately downstream of the guard pinhole, an in-vacuum cryochamber (Microstat He, Oxford Instruments, Oxon, UK) was placed on a three-axis goniometer. Its windows had been replaced by thin Kapton films. Both the distance between the two pinholes and that between the guard pinhole and the specimen were  $\sim 8$  mm. The specimen-to-detector distance was 3.26 m, and the detector was a cooled CCD camera (C 4880, Hamamatsu Photonics, Hamamatsu, Japan) in combination with an image intensifier (VP 5445, Hamamatsu Photonics) with P46 phosphor (Yagi *et al.*, 2004).

The conventional recordings from single muscle fibers were carried out at the BL45XU beamline (small-angle scattering station) of SPring-8. The set-up was identical to that of BL40XU except that the pinhole optics was omitted, the specimen-to-detector distance was 2 m and the image intensifier was P43 phosphor. The energy of the X-ray beam was 13.8 keV and its resolution was  $10^{-4}$ .

## 2.2. Materials

The material used as an example for the microdiffraction was the myofibrils prepared from the longitudinal flight muscle of a bumblebee, *Bombus* sp. The muscle was first glycerinated in a 50% mixture of glycerol and a relaxing

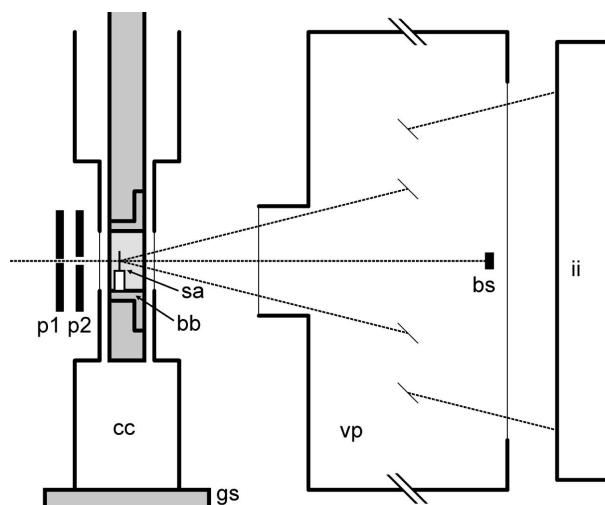


**Figure 1**  
Schematic diagram for the arrangement of optics. p1, defining pinhole; p2, guard pinhole; sa, sample grid; bb, brass block; cc, in-vacuum cryochamber with Kapton windows; gs, three-axis goniometer stage; vp, vacuum path; bs, tantalum beamstop; ii, image intensifier and CCD detector.

solution with a composition described by Iwamoto (1995), and was stored in the same solution at 253 K until used. The muscle fibers were then isolated, suspended in a rigor solution [described by Iwamoto (2000), but also containing 20% 2-methyl-2,4-pentanediol as a cryoprotectant] and homogenized using a Polytron homogenizer (model PT10/35, Polytron, Littau, Switzerland) to obtain a suspension of myofibrils. For the material for conventional diffraction recording, isolated single skinned skeletal muscle fibers of rabbit were used, prepared as described by Iwamoto (1995).

## 2.3. Quick freezing

A small drop of myofibril suspension was placed on a copper grid for electron microscopy covered with a thin Kapton film, whose surface had been pre-treated with poly L-lysine. The isolated single muscle fiber was also mounted on a grid, on which a narrow slit had been cut out to accommodate the fiber. The fiber was mounted in the relaxing solution, and then transferred to the rigor solution with 20% methyl pentanediol. In either case, the grids were blotted, and plunged into liquid propane cooled to  $\sim 93$  K by using a quick-freezing apparatus for electron microscopy (EM-CPC, Leica, Heerbrugg, Switzerland). The specimens frozen in this way were stored in liquid nitrogen until X-ray recording.

## 2.4. X-ray diffraction recording

Immediately before transfer to the pre-cooled cryochamber, the grids were affixed to a brass block pre-cooled to the liquid-nitrogen temperature. The brass block was designed to fit into the copper specimen holder of the cryochamber. The cryochamber was briefly opened in a nitrogen atmosphere to transfer the specimen. Because the long copper specimen holder was a source of thermal drift, the vertical position of the holder was constantly monitored during X-ray recording by a laser displacement sensor (model LC-2440, Keyence, Osaka, Japan) and was compensated with an accuracy of 0.5  $\mu\text{m}$ . To scan the grids with respect to the beam, the whole cryochamber was moved in the horizontal and vertical directions.

## 3. Results and discussion

### 3.1. Microbeam profile

The profile of the microbeam at the sample position was obtained by differentiating the knife-edge scan record. The profile shows that the full width at half-maximum (FWHM) was 1.5  $\mu\text{m}$  (Fig. 2). The estimated flux of the 1/100-attenuated microbeam was  $5 \times 10^9$  photons  $\text{s}^{-1}$  as measured using a large-area PIN photodiode. In BL45XU, a FWHM of 0.9  $\mu\text{m}$  was obtained (Iwamoto, Nishikawa *et al.*, 2002).

### 3.2. Resolution of the microbeam

Fig. 3 shows the pattern recorded from chicken tendon collagen, to evaluate the resolution obtained from the microbeam. The first-order reflection (at  $1/65 \text{ nm}^{-1}$ ) is readily

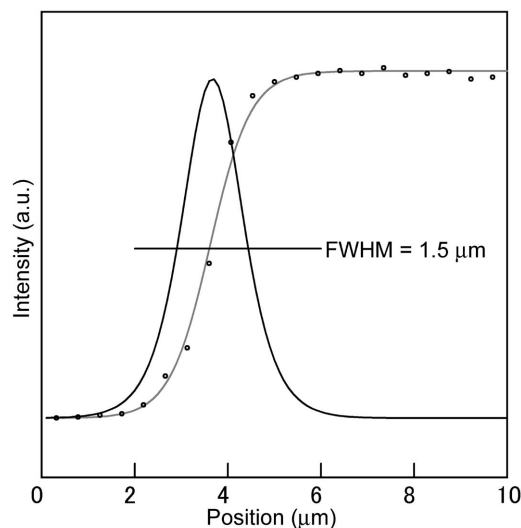


**Figure 2**

Knife-edge scan of the microbeam generated at BL40XU. The recorded intensities are fitted to a sigmoidal function and then differentiated to obtain the beam profile. The full width at half-maximum (FWHM) is 1.5  $\mu\text{m}$ .

resolved, and the small-angle resolution should be at least  $1/100 \text{ nm}^{-1}$ . Owing to Fraunhofer diffraction, the microbeam is expected to spread, depending on the size of the defining aperture and X-ray energy. The extent of the spread, expressed as the radius of the airy disk at the detector, is estimated to be  $\sim 180 \mu\text{m}$ , *i.e.* comparable with the pixel size of the detector (200  $\mu\text{m}$ ). Therefore, it is concluded that Fraunhofer diffraction does not significantly affect the quality of microdiffraction patterns. Although there is no gain in flux density, the pinhole optics is considered more suitable for small-angle scattering applications than condensing optics (*e.g.* zone plates and a pair of mirrors in the Kirkpatrick–Baez configuration), in that more parallel beams can be generated.

### 3.3. Microdiffraction from an isolated myofibril

A macroscopic specimen of muscle or muscle fiber (diameter  $\sim 100 \mu\text{m}$  or greater) contains a large number of myofibrils (diameter  $\sim 3 \mu\text{m}$  in insect flight muscle). A single myofibril consists of  $\sim 3 \mu\text{m}$  repeating units called sarcomeres. In each sarcomere, the myofilaments (actin-containing thin filaments and myosin-containing thick filaments) are arranged in a hexagonal lattice. This lattice arrangement should give rise to a series of ‘equatorial reflections’ indexable to the hexagonal lattice, which are essentially Bragg reflections. In insect flight muscle, the strongest of all are the 1,0 and 2,0 reflections. Because different myofibrils have different lattice plane orientations, the diffraction pattern is basically a ‘powder diffraction’, which contains reflections of all combinations of lattice indices  $h$  and  $k$  (see Iwamoto, Nishikawa *et al.*, 2002).

However, a single sarcomere of an isolated myofibril contains only one hexagonal lattice. Therefore, reflections would arise only when the lattice plane meets the Bragg

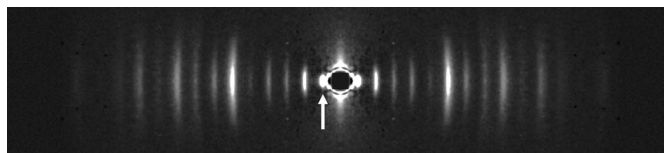


**Figure 3**

Microdiffraction pattern recorded from chicken tendon collagen cooled to 74.5 K. Exposure time, 2 s. The arrow indicates the first-order reflection at  $1/65 \text{ nm}^{-1}$ .

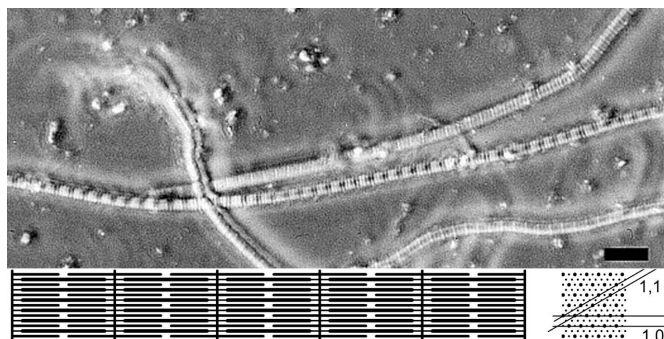


**Figure 4**

Phase-contrast light microscopic image of the suspension of myofibrils prepared from a bumblebee flight muscle, observed by using an Olympus IX-70 inverted microscope. Repeating sarcomeres (minimal functional units of muscle) can be observed. Scale bar, 10  $\mu\text{m}$ . The drawing below is a schematic diagram of the structure of an insect flight muscle myofibril. The 1,0 and 1,1 planes are indicated in the cross section.

condition, if a diffraction pattern is recorded from a single sarcomere.

A micrograph of the insect flight muscle myofibril preparation is shown in Fig. 4. Although a large number of myofibrils should be adsorbed onto the grid surface, diffraction patterns from them were rarely observed. This is expected, because relatively few of the lattices would meet the Bragg conditions to generate strong reflections from the 1,0 lattice plane.

An example of a series of microdiffraction patterns is shown in Fig. 5(a). These patterns were recorded by scanning the grid, in the direction almost perpendicular to the myofibril axis, with a step of 1  $\mu\text{m}$ . The reflection angles of the two strong reflections correspond to those of the 1,0 and 2,0 equatorial reflections. The intensity profile along the equator (Fig. 5b) shows the total lack of the 1,1 reflection, which would be observed along with the 1,0 and 2,0 reflections in the pattern from the whole fiber preparation or in the ‘end-on’ diffraction pattern (Iwamoto, Nishikawa *et al.*, 2002). This reflects the fact that, when the 1,0 lattice plane meets the Bragg condition, the 1,1 plane never does so, and indicates that the pattern genuinely originated from a single hexagonal lattice. The much weaker meridional reflections were not observed.

The isolated myofibrils are usually tens of micrometers long, but it was impossible to track the myofibril by following the reflections; a very confined stretch of the myofibril seemed to generate the reflections. This could occur if the myofibril was slightly twisted when it was adsorbed onto the grid, and the

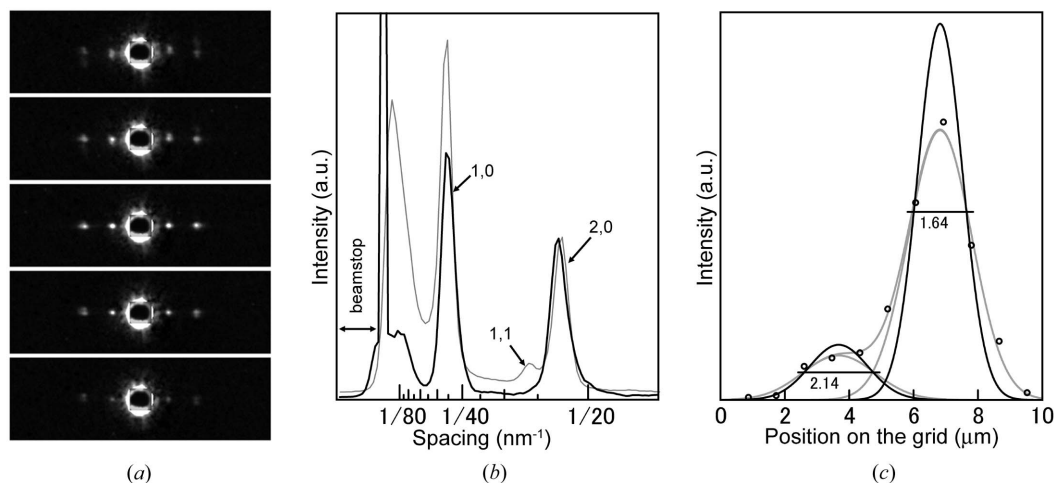


**Figure 5** Microdiffraction pattern recorded from a quick-frozen myofibril of bumblebee flight muscle. (a) A series of diffraction patterns recorded by scanning the grid in the direction at  $60^\circ$  to the myofibril axis with  $1 \mu\text{m}$  steps. Exposure time, 10 s each. (b) Intensity profile of the diffraction pattern measured along the equator. Black line, profile taken from one (middle) of the microdiffraction patterns in (a). Gray line, profile obtained from an end-on (powder) diffraction pattern recorded with a  $50 \mu\text{m}$  pinhole (Iwamoto, Nishikawa *et al.*, 2002). The lack of the 1,1 reflection is evident in the profile taken from a single myofibril. (c) Intensity of the 2,0 reflection as a function of position on the grid, measured across the myofibrillar axis. Circles represent the measured data, which can be fitted to a sum of two Gaussian distributions (gray line). Solid lines are the distributions corrected for the beam width (Fig. 2) by deconvolution. The values indicated beneath the horizontal lines are the FWHMs of the two distributions.

lattice met the Bragg condition only in a limited number of sarcomeres.

Fig. 5(c) shows the integrated intensity of the strong 2,0 reflection as a function of position on the grid, as obtained by scanning the grid across the myofibril axis. The profile represents the convolution between the projection of the myofibril cross section and the beam profile as indicated in Fig. 2. The intensity profile can be fitted to a sum of two Gaussian distributions, weak and strong. The weaker set of reflections appeared at an angle slightly different from that of the stronger set, suggesting that there were either two myofibrils close to each other or a single partially broken (unevenly split) myofibril. After correction for the beam width as shown in Fig. 2, the FWHMs of the two distributions are  $1.64 \mu\text{m}$  and  $2.14 \mu\text{m}$  for the strong and weak peaks, respectively. From these, the diameters of the myofibrils are estimated to be  $1.89 \mu\text{m}$  and  $2.47 \mu\text{m}$ , respectively (after dividing by  $\sqrt{3}/2$ , by assuming that the myofibrils have a circular cross section), and  $2.68$  and  $3.49 \mu\text{m}$ , respectively, after taking the square law into consideration. These values coincide with the diameter of the myofibrils of asynchronous flight muscle ( $\sim 3 \mu\text{m}$ ). This result further confirms the idea that the reflections originated from single myofibrils. Because of the circular profile of the beam, the size of the area irradiated by the microbeam should be equivalent to that of a single sarcomere ( $\sim 3 \mu\text{m}$  long).

Finally, the conventional diffraction pattern from a quick-frozen single skeletal muscle fiber is shown in Fig. 6. Besides the strong equatorial reflections (attenuated by a copper mask), weaker myosin-based meridional reflections and actin-based layer-line reflections are clearly observed, including the faint outer part of the 'second actin layer line' believed to originate from tropomyosin (one of the regulatory proteins on the thin filament). An array of 30 unfrozen single fibers would be needed to observe this faint reflection clearly (Iwamoto *et*

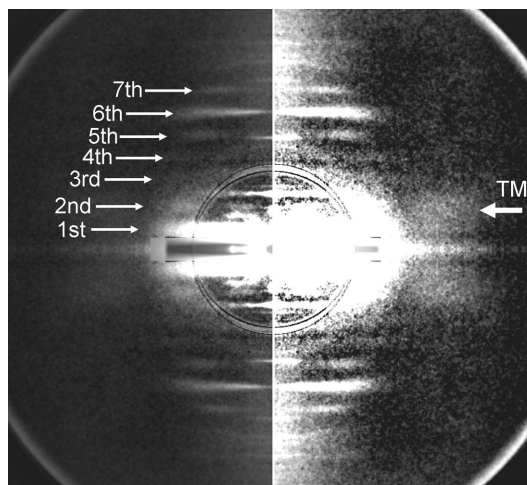


**Figure 6** Conventional diffraction pattern from a quick-frozen single skeletal muscle fiber in rigor, recorded at BL45XU. Background scattering has been subtracted according to the method described by Iwamoto *et al.* (2003). The right half of the pattern is shown with a higher gain. The black overlapping rings at the center are due to the correction for a circular aluminium mask to attenuate the central intense part of the diffraction pattern. The outer whitish ring is due to the background subtraction. The four quadrants of the diffraction pattern have been folded. Note that a number of actin-based layer-line reflections (first to seventh) are clearly visible (arrows), including the faint outer second actin layer line reflection (TM). Total exposure time, 500 s.

*al.*, 2001; Iwamoto, Oiwa *et al.*, 2002; Tamura *et al.*, 2004; Wakayama *et al.*, 2004). Therefore, it is remarkable that such a diffraction pattern can be obtained from a  $1/30$  volume of specimen if it is properly quick-frozen. The stability and the resistance to radiation damage of the specimen are also remarkable, since the fiber withstood a total of 500 s exposure time without noticeable deterioration of the pattern, while

unfrozen fiber would withstand an exposure time of less than 10 s with the same beam intensity.

#### 4. Conclusion

Overall, the present results demonstrate the vast potential of the quick-freezing and recording-while-frozen technique in both microdiffraction and conventional diffraction applications. In the former it is demonstrated that a diffraction pattern can be recorded from a hydrated biological specimen as small as  $\sim 10 \mu\text{m}^3$  in volume. In the latter application the amount of specimen needed for recording can also be greatly reduced. In addition, it makes it possible to quick-freeze a specimen at a desired moment of reaction and observe its structure. The combination of the present freezing technique and the bright low-emittance source of synchrotron radiation promises a greater possibility of structural analysis by means of X-ray diffraction in the field of life sciences.

This work was conducted under approval of the SPring-8 Proposal Review Committee (Proposal Nos. 2003B0189; 2004A0583; 2004A0584; 2004B0474). Supported by Grant-in-Aid, Grant No. 15500294, Ministry of Education, Culture, Sports, Science and Technology and Special Coordination Funds of the Ministry of Education, Culture, Sports, Science and Technology, Japan.

#### References

- Busson, B., Engström, P. & Doucet, J. (1999). *J. Synchrotron Rad.* **6**, 1021–1030.
- Ice, G. E. (1997). *X-ray Spectrom.* **26**, 315–326.
- Inoue, K., Oka, T., Suzuki, T., Yagi, N., Takeshita, K., Goto, S. & Ishikawa, T. (2001). *Nucl. Instrum. Methods Phys. Res. A*, **467/468**, 674–677.
- Iwamoto, H. (1995). *Biophys. J.* **68**, 243–250.
- Iwamoto, H. (2000). *Biophys. J.* **78**, 3138–3149.
- Iwamoto, H., Nishikawa, Y., Wakayama, J. & Fujisawa, T. (2002). *Biophys. J.* **83**, 1074–1081.
- Iwamoto, H., Oiwa, K., Suzuki, T. & Fujisawa, T. (2001). *J. Mol. Biol.* **305**, 863–874.
- Iwamoto, H., Oiwa, K., Suzuki, T. & Fujisawa, T. (2002). *J. Mol. Biol.* **317**, 707–720.
- Iwamoto, H., Wakayama, J., Fujisawa, T. & Yagi, N. (2003). *Biophys. J.* **85**, 2492–2506.
- Kreplak, L., Franbourg, A., Briki, F., Leroy, F., Dalle, D. & Doucet, J. (2002). *Biophys. J.* **82**, 2265–2274.
- Lichtenegger, H., Muller, M., Paris, O., Riekkel, C. & Fratzl, P. (1999). *J. Appl. Cryst.* **32**, 1127–1133.
- Riekkel, C., Burghammer, M. & Müller, M. J. (2000). *J. Appl. Cryst.* **33**, 421–423.
- Rossle, M., Panine, P., Urban, V. S. & Riekkel, C. (2004). *Biopolymers*, **74**, 316–327.
- Tamura, N., MacDowell, A. A., Spolenak, R., Valek, B. C., Bravman, J. C., Brown, W. L., Celestre, R. S., Padmore, H. A., Batterman, B. W. & Patel, J. R. (2003). *J. Synchrotron Rad.* **10**, 137–143.
- Tamura, T., Wakayama, J., Fujisawa, T., Yagi, N. & Iwamoto, H. (2004). *J. Muscle Res. Cell Motil.* **25**, 329–335.
- Wakayama, J., Tamura, T., Yagi, N. & Iwamoto, H. (2004). *Biophys. J.* **87**, 430–441.
- Yagi, N., Inoue, K. & Oka, T. (2004). *J. Synchrotron Rad.* **11**, 456–461.